Journal of Applied Polymer Science

Synthesis and characterization of a ferrocene-modified, polyaniline-like conducting polymer

Yunlong Li,[1,2] Yuying Zheng[1]

[1]College of Materials Science and Engineering, Fuzhou University, Fuzhou 350116, China
[2]Department of Light-Textile Engineering, Liming Vocational University, Quanzhou 362000, China
Correspondence to: Y. Zheng (E-mail: ylli@lmu.edu.com)

ABSTRACT: A novel monomer called *1,1′-ferrocenediacyl anilide* (FcA) was synthesized from ferrocene (Fc). Copolymerization was carried out between FcA and aniline (ANI) by an electrochemical method. The novel monomer and copolymer were characterized with ^{1}H-NMR, Fourier transform infrared (FTIR) spectroscopy, and ultraviolet–visible (UV–vis) spectroscopy. The hydrogen protons of the benzene ring were moved to a low field in ^{1}H-NMR, and the absorption band of N═Q═N (where Q is the quinoid ring) appeared in the FTIR spectrum of the polymer. The peaks of both Fc and the π–π^* electronic transition in the UV–vis spectra were redshifted. The results indicate that the copolymer mainly existed as a highly delocalized conjugated system. X-ray diffraction analysis established further proof, and the process of electrochemical deposition was observed by scanning electron microscopy. The optimal synthesis conditions of the copolymer were determined through changes in the monomer molar ratios and the scan rate. The ideal performance of the copolymer was gained when the monomer molar ratio between FcA and ANI was 1:4 and the scan rate was 50 mV/s. Furthermore, the electrochemical performances were tested in detail by cyclic voltammetry, galvanostatic charge–discharge testing, and electrochemical impedance spectroscopy. The results show that the specific capacitance of poly(1,1′-ferrocenediacyl anilide-*co*-aniline) increased up to 433.1 F/g at 0.5 A/g, the diffusion resistance was very small, and the durability was good enough. © 2015 Wiley Periodicals, Inc. J. Appl. Polym. Sci. **2016**, *133*, 43217.

KEYWORDS: conducting polymers; electrochemistry; properties and characterization

Received 26 August 2015; accepted 9 November 2015
DOI: 10.1002/app.43217

INTRODUCTION

The conducting polymer, as a new cross-subject research field, has been widely investigated by physical scientists, chemists, and material scientists all over the world.[1–6] Among conducting polymers, polyaniline (PANI) and its derivatives are unique because of their good environmental stability and controllable electrical properties, and they are used in a vast range of applications, such as organic lightweight batteries, electrochromic displays, solar cells, and electroluminescent and sensor elements.[7–13] However, PANI has a defective site[14,15] and exhibits an ill-defined structure, and the conducting electricity of PANI is activated in acid medium. Therefore, many ways have been presented to solved the problem,[16–20] including the production of a composite with a metal oxide and carbon materials and modification of the polymer.

Organometallic compounds are also a hotspot because of their characteristics of electron delocalization; this gives them unique electricity, magnetism, light, and other properties.[21–23] Ferrocene (Fc) and its derivative modified electrodes have mainly been applied in the fields of electrocatalysis, electroanalysis, and biosensors. The Fc-based polymer is one metal-containing polymer that has been shown to possess some unique physical and chemical properties because its particular chemical structure is similar to that of the composite of the polymer and metal. Well-defined Fc-containing polymers were reported first in 1972.[24] Then, Fc-based conducting polymers were the hotspot because of the redox properties of both groups of this kind of polymer.[25] Also, they were proven to be effective in improving the electrochemical performances of conducting polymers when Fc was on the main conjugation path of the polymer backbone.[26,27] This field has been an attractive area of research for multiapplications in recent years.[28,29]

In this study, a novel electroactive copolymer was prepared by electrochemical polymerization; this copolymer possessed difunctional Fc in the main chain. Furthermore, ^{1}H-NMR, Fourier transform infrared (FTIR), X-ray diffraction (XRD), and scanning electron microscopy (SEM) were used to characterize the product, and the electrochemical properties were studied in detail.

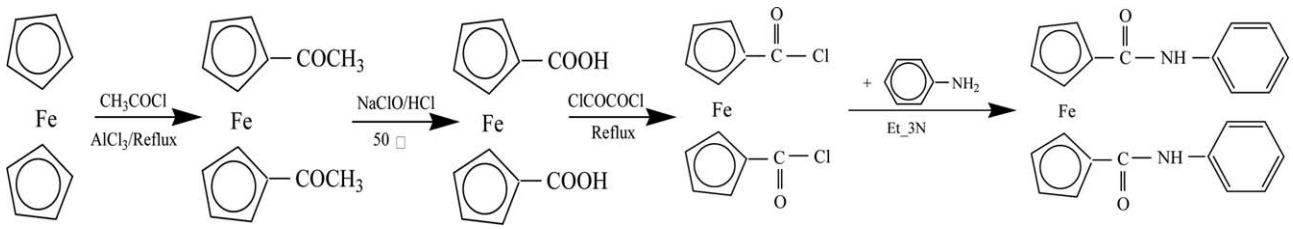

Scheme 1. Synthesis of FcA from Fc.

EXPERIMENTAL

Materials

Ferrocene (Fc), aluminum chloride ($AlCl_3$), acetyl chloride (CH_3COCl), oxalyl chloride, and aniline (ANI) were provided by Shanghai Chemical Industry. Ethanol, sodium hydroxide, sodium hypochlorite (NaClO) solution, sodium hydrogen sulfite, sodium carbonate (crystal), triethylamine (Et_3N), concentrated hydrochloric acid (HCl), and perchloric acid were purchased from Guangxi Chemistry Industry. Other chemicals, including concentrated sulfuric acid and *N,N′*-dimethylformamide, were purchased from the Chemical Plant of Chinese Curatorial Group. All of the chemicals were reagent grade and were used without further purification.

Synthesis of 1,1′-Ferrocenediacyl Anilide (FcA)

As shown in Scheme 1, FcA was produced by the interaction between 1,1′-ferrocene dicabonyl chloride and ANI. Suitable preparation methods for 1,1′-ferrocenediacyl chloride, 1,1′-ferrocene dicarboxylic acid, and 1,1′-diacetyl ferrocene were reported in the literature.[30]

A solution of 30 mmol of 1,1′-ferrocene dicarbonyl chloride in 200 mL of dry methylene chloride was added dropwise (1 drop/s) to a stirring mixture of 60 mmol of ANI and 20 mL of Et_3N in 200 mL of methylene chloride. The reaction proceeded readily at room temperature (ca. 25°C) and was stirred for 3 h. The product was precipitated as a fine brown crumb, and the mixture was filtered from the solution; then, the filter cake was washed three times with methylene chloride, ammonium hydroxide, and diethyl ethers, respectively. Finally, the product was dried in a vacuum oven at 30°C for 24 h. The yield of the product was about 85%.

Synthesis of Poly(1,1′-ferrocenediacyl anilide-*co*-aniline) [P(FcA-*co*-ANI)]

The synthesis route of the FcA and ANI copolymer [P(FcA-*co*-ANI)] is illustrated in Scheme 2. The novel electroactive polymer was synthesized from the reaction of FcA and ANI by electrochemical polymerization with the cyclic voltammetry method at 10°C. In this way, the copolymer, with a nondefective conjugated structure, was easy to separate and purify.

The reaction was performed with a three-electrode method, with a foaming nickel net (1 × 1 cm^2) as a working electrode, a platinum sheet as a counter electrode, and an Ag/AgCl electrode as the reference electrode, respectively. The potential limit was between −0.2 and 1.2 V, and the scan rates were 10, 20, 50, 100, and 200 mV/s. FcA and ANI were dissolved in the electrolyte (1 mol/L of $HClO_4$), and the monomer molar ratios (FcA/ANI) were 1:1, 1:2, 1:3, 1:4, and 1:5, respectively.

Characterization of the Monomer and the Polymer

^{1}H-NMR Analysis. The ^{1}H-NMR spectra of FcA and P(FcA-*co*-ANI) were obtained on a Bruker ARX 300-MHz spectrometer with 1000 scans at a relaxation time of 2 s with hexadeuterated dimethyl sulfoxide (d_6-DMSO) as the solvent.

FTIR Analysis. The samples were measured with FTIR spectroscopy (Nicolet Magna-IR 750 spectrometer) after the KBr disc and samples were pressed.

Ultraviolet–Visible (UV–vis) Absorption Analysis. The samples were analyzed with a UV-2501 PC spectrometer (Shimadzu) from 200 to 800 nm with dimethylformamide as the solvent.

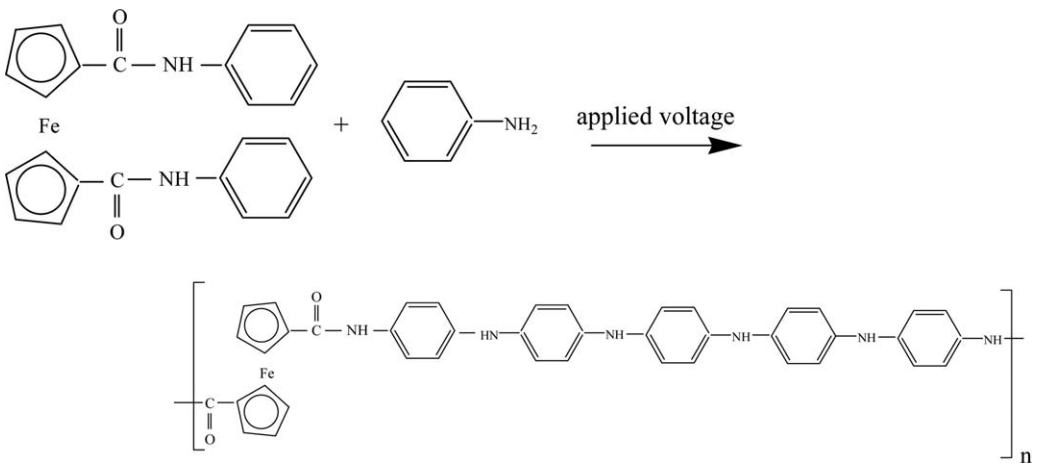

Scheme 2. Synthesis of P(FcA-*co*-ANI).

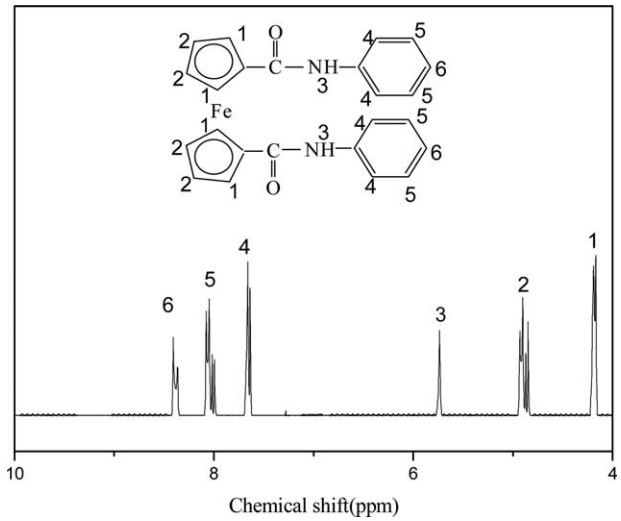

Figure 1. ^{1}H-NMR spectrum of FcA in d_6-DMSO.

XRD Analysis. The samples were measured with an X-ray powder diffractometer (D8 Advanced) after they were ground into powder. The scan range was 2–100°.

SEM Analysis. The surface morphology of the copolymer was measured with a LEO-1530 scanning electron microscope.

Electrochemical Experiments

All electrochemical experiments were measured by a three-electrode system in 1 mol/L $HClO_4$ electrolyte with a CHI600D electrochemical work station (Chenhua, Shanghai). The counter and reference electrodes were with a platinum sheet and Ag/AgCl, respectively. The working electrode was prepared by electrochemical deposition onto a foaming nickel net (1 × 1 cm^2).

RESULTS AND DISCUSSION

Characterization of the Monomer and the Copolymer

^{1}H-NMR Analysis of the Monomer and the Copolymer. Figure 1 shows the ^{1}H-NMR spectrum of FcA. The peaks at 4.15–4.23 and 4.82–4.93 ppm were assigned to α-H (4H) and β-H (4H) of bis-substituted Fc. The tertiary amino

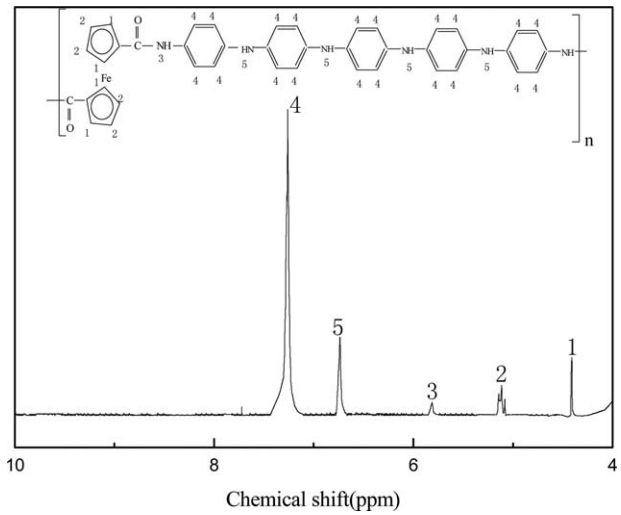

Figure 2. ^{1}H-NMR spectrum of P(FcA-*co*-ANI) in d_6-DMSO.

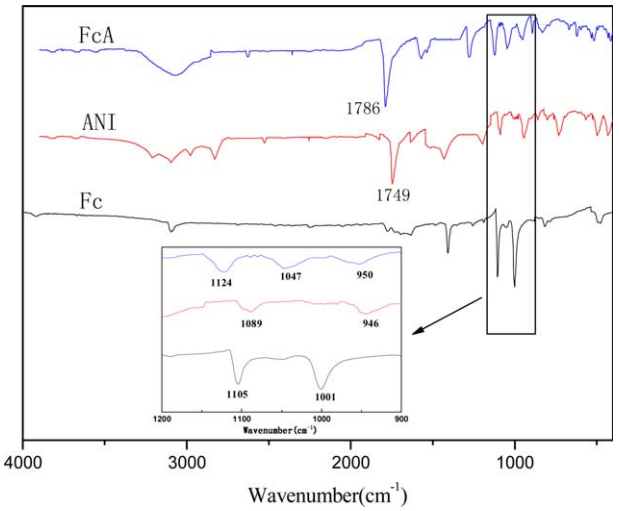

Figure 3. FTIR spectra of Fc, ANI, and FcA. [Color figure can be viewed in the online issue, which is available at wileyonlinelibrary.com.]

peak (—NH—) in FcA appeared at 5.73 ppm. The peaks at 7.63–7.73, 7.97–8.10, and 8.34–8.41 ppm were assigned to α-H (4H), β-H (4H), and γ-H (2H), respectively, of the anilino group. They moved to a low field compared with the hydrogen protons of the benzene ring (7.25 ppm) because of a conjugative effect.

^{1}H-NMR analysis of the copolymer was performed to confirm the structure, as shown in Figure 2. The peaks at 4.41 and 5.11 ppm were attributed to the protons of the ferrocenyl segments, which moved to a low field compared with the value of FcA because of a conjugative effect. The signals at 5.82 and 6.74 ppm were ascribed to the two kinds of amino protons, respectively. Furthermore, the signal at about 7.26 ppm was ascribed to the protons of the benzene ring; we assumed absolute superiority in the hydrogen content of the copolymer.

FTIR Analysis of the Monomer and the Copolymer. The FTIR spectra of Fc, ANI, and FcA were illustrated in Figure 3. In the spectrum of FcA, the absorption band at 3076 cm^{-1} was assigned to N—H stretching vibrations, and the peak at 1786 cm^{-1} was attributed to C═O stretching. The peak at 1570 cm^{-1} was attributed to the stretching vibrations of benzene rings. The vibrations at 1276 cm^{-1} were attributed to the C—N stretching vibrations that arose from secondary aromatic amine groups. All of the peaks appeared on the FTIR spectrum of ANI at similar positions. Furthermore, the signals at 1124, 1047, and 956 cm^{-1} in the spectrum of FcA were characteristic absorption peaks of ferrocenyl rings and benzene rings. The symmetric peaks at 1105 and 1001 cm^{-1} in spectrum of Fc were characteristic absorption peaks of ferrocenyl rings, and the peaks at 1089 and 946 cm^{-1} corresponded to out-of-plane and in-plane vibrations of the benzene ring.

To confirm the structure of P(FcA-*co*-ANI), the FTIR spectra of FcA, PANI, and P(FcA-*co*-ANI) were obtained, as depicted in Figure 4. Compared with the spectrum of FcA, there were similar peaks at wave numbers higher than 1600 cm^{-1} in the FTIR spectrum of P(FcA-*co*-ANI). However, the peak at 1467 cm^{-1}

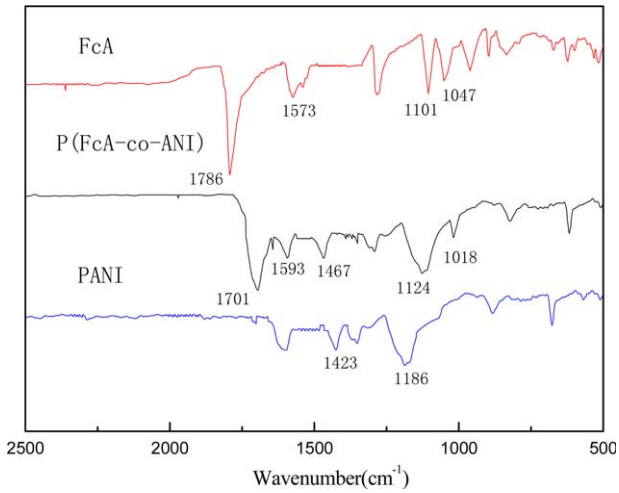

Figure 4. FTIR spectra of FcA, PANI, and P(FcA-*co*-ANI). [Color figure can be viewed in the online issue, which is available at wileyonlinelibrary.com.]

was from N—B—N (where B is the benzene ring). The peaks at 1129 and 1018 cm^{-1} became asymmetric, and the absorption band at 1129 cm^{-1} became stronger than the similar peak in the spectrum of FcA, this was due to N=Q=N (where Q is the quinoid ring)[31] and perchlorate anion incorporation in copolymer.[32] The characteristic absorption peaks almost appeared in the case of pure PANI. The results indicated that the molecular units of the copolymer contained a highly delocalized conjugated system; the formation of copolymer was shown in Scheme 3.

UV–Vis Absorption Analysis of the Monomer and Copolymer. The UV–vis spectra of Fc, FcA, and P(FcA-*co*-ANI) were shown in Figure 5. The first absorption peak of Fc at 250 nm was observed, this was associated with the characteristic Fc structure, and the absorption peak was redshifted in the spectra of FcA (252 nm) and P(FcA-*co*-ANI) (254 nm). It was influenced by the π–π^* conjugated system between the ANI and ferrocenyl segments. Meanwhile, the absorption peaks of the π–π^* electronic transition[33] appeared 316 nm in the spectrum of FcA and redshifted to 325 nm in the spectrum of P(FcA-*co*-ANI) because of the higher conjugation effects.

XRD Analysis of the Polymer. The XRD curve of P(Fca-*co*-ANI) is depicted in Figure 6, the diffuse peak present in the curve indicated that the product obtained was the amorphous polymer. There were two peaks present in the curve. The intense peak centered at about 18° was mainly due to the periodicity parallel to the polymer chain, and that at about 28° was ascribed to the periodicity perpendicular to the chain direction.[34] Compared with the PANI–β-naphthalene sulfonic acid microtubes, which possessed a high crystallinity, it was quite different. This was mainly due to the special stereochemistry structure and conjugated segment in the main chain of P(FcA-*co*-ANI).

SEM Analysis of the Copolymer. Figure 7 showed the SEM images of P(FcA-*co*-ANI) through electrochemical polymerization.

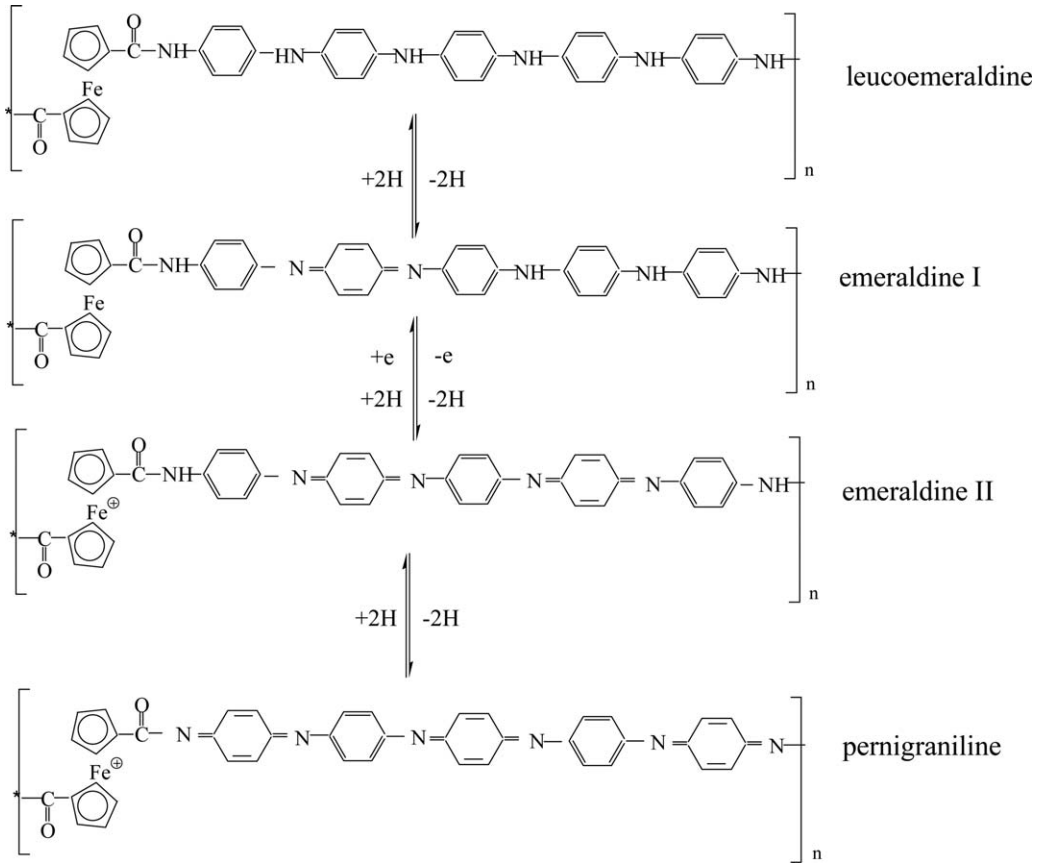

Scheme 3. Molecular structures of P(FcA-*co*-ANI) at various oxidation states.

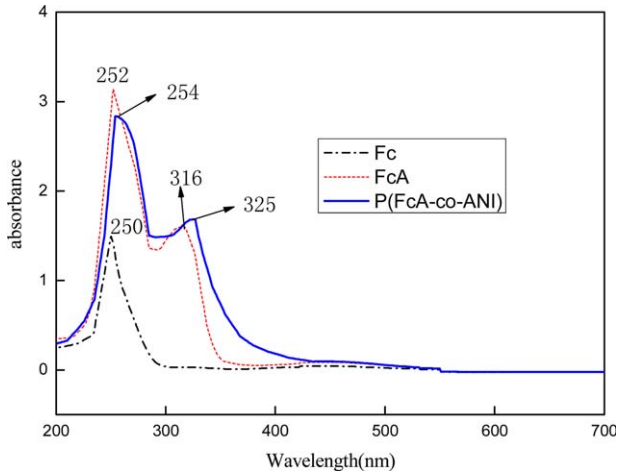

Figure 5. UV–vis absorption spectra of Fc, FcA, and P(FcA-*co*-ANI). [Color figure can be viewed in the online issue, which is available at wileyonlinelibrary.com.]

The copolymer had a small rod shape and was spherical at the beginning; then, it gradually gathered to form island structures, which covered the surface of the foaming nickel evenly after a long deposition time. This morphology had large specific surface, which contributed to the improvement of the electrochemical properties of the copolymer.

Optimization of the Synthesis Conditions

To gain the optimal synthesized conditions of copolymer, the effects of the monomer molar ratios and scan rate were examined through the specific capacitance (C_s; F/g), respectively. C_s was determined from the charge–discharge curves and was calculated according to the following equation:

$$C_s = \frac{I\Delta t}{\Delta V m}$$

where ΔV (v), m (g), I (A), and Δt (s) were the potential window in the charge–discharge curve, mass of the active material, discharge current, and time, respectively.

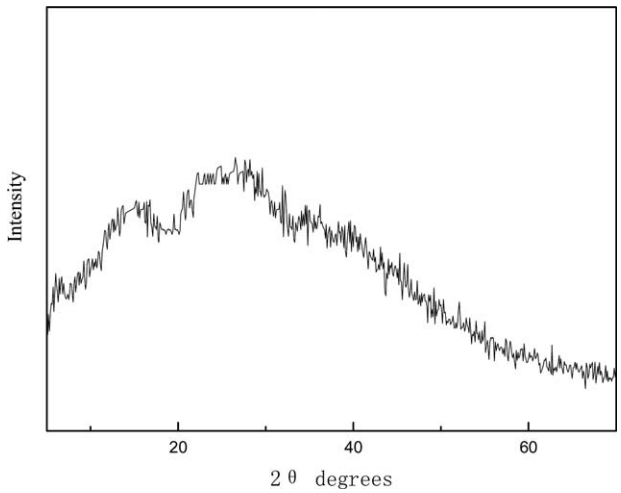

Figure 6. XRD curve of P(FcA-*co*-ANI).

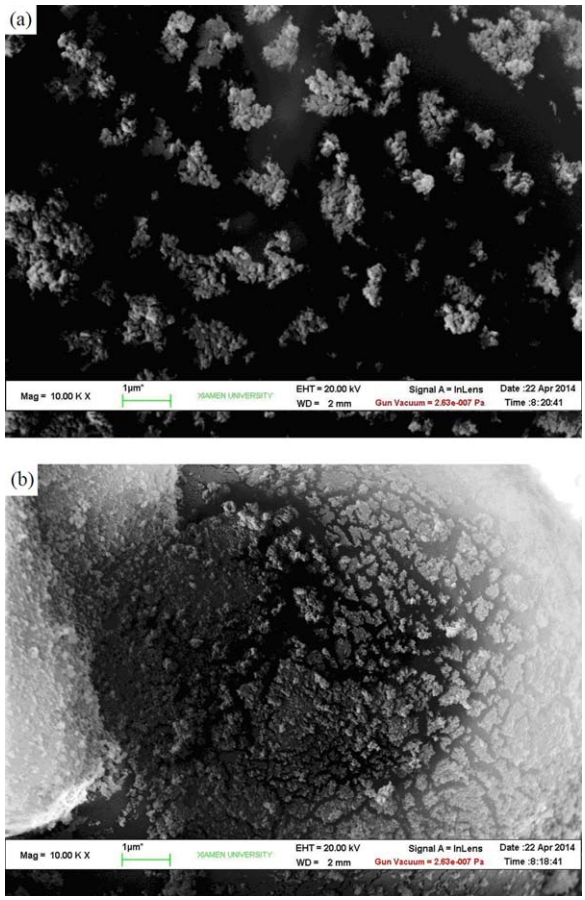

Figure 7. SEM images of P(FcA-*co*-ANI) for different polymerization times: (a) 15 and (b) 60 min. [Color figure can be viewed in the online issue, which is available at wileyonlinelibrary.com.]

The charge–discharge curves at different monomer molar ratios were depicted in Figure 8, and the calculated values of each curve were shown in Table I. The results show that the copolymer had good capacitive behavior at large-scale current densities because of the nearly symmetric charge–discharge curves. As

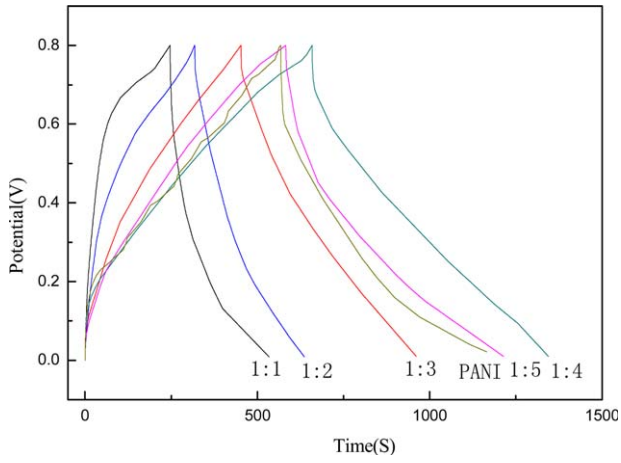

Figure 8. Charge–discharge curves at different monomer molar ratios at 0.5 A/g. [Color figure can be viewed in the online issue, which is available at wileyonlinelibrary.com.]

Table I. C_s Values of Samples with Different Monomer Molar Ratios

Monomer molar ratio (FcA/ANI)	1:1	1:2	1:3	1:4	1:5	Pure PANI
C_s (F/g)	165.8	198.8	300.3	433.1	381.8	373.8

shown in Figure 8 and Table I, with increasing ratio of ANI, C_s increased first and then decreased, and the maximum value was gained when the monomer molar ratio between FcA and ANI was 1:4. The maximum C_s (433.1 F/g) was higher than that of pure PANI (373.8 F/g). This result could be explained by the following factors. First, the copolymerization between FcA and ANI was blocked by the steric hindrance of FcA. Therefore, the raised ratio of FcA restricted electrolyte ion-transmission paths. Second, the ideal conjugated structure formed with a suitable dosage of FcA, as shown in Scheme 2.

The influence of the scan rates on the charge–discharge curves are shown in Figure 9, and the calculated values of each curve are shown in Table II. The results showed that C_s increased with increasing scan rate. However, there was a limit to the scan rate, as shown in Table II, where a more than 50 mV/s disinfection increase was not obvious. Furthermore, it was clearly seen that the internal resistance (IR) increased with the increasing of scan rates, and the less "IR" was signified the lower internal resistance of the electrode. This result illustrated that the copolymerization rates were in inverse proportion to "IR", and the integrated performance of P(FcA-co-ANI) was gained at the scan rate of 50 mv/s.

Electrochemical Properties of the Copolymer

To further explore its application as a supercapacitor electrode, the electrochemical performance of P(FcA-*co*-ANI) was tested by cyclic voltammetry (CV), galvanostatic charge–discharge testing, and electrochemical impedance spectroscopy (EIS). The CV curves were depicted in Figure 10. Three pairs of conspicuous peaks were obvious in the CV curves. The peaks at a, b, and c

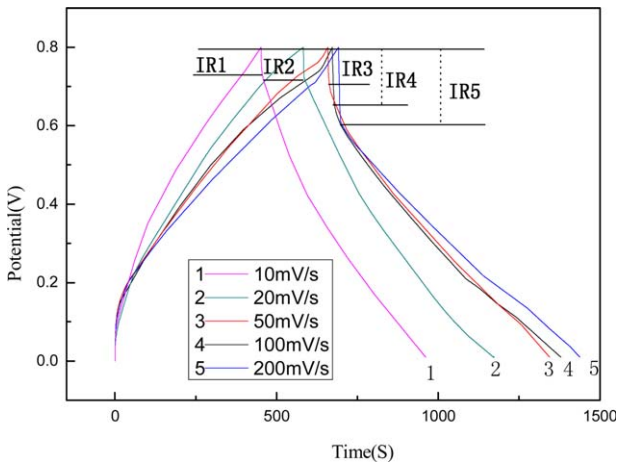

Figure 9. Charge–discharge curves at different scan rates at 0.5 A/g. The internal resistance (IR) was determined from the voltage drop at the beginning of each discharge, and the slope of voltage drop was very close to zero. [Color figure can be viewed in the online issue, which is available at wileyonlinelibrary.com.]

Table II. C_s Values of Samples with Different Scan Rates

Scan rate (mV/s)	10	20	50	100	200
C_s (F/g)	300.3	364.8	433.1	446.3	452.6

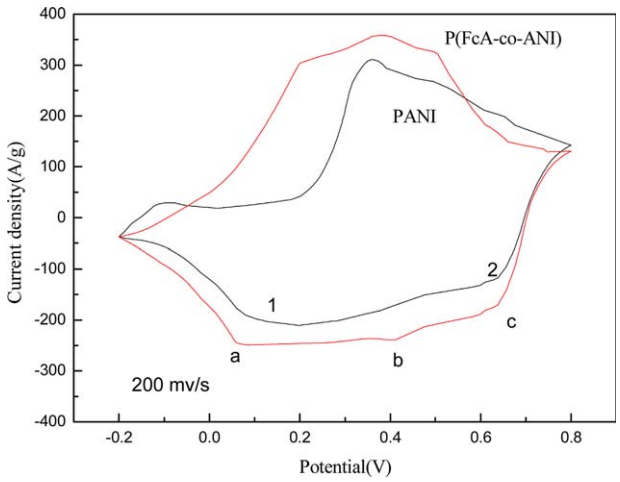

Figure 10. CV curves of P(FcA-*co*-ANI) and PANI at a scan rate of 200 mV/s. [Color figure can be viewed in the online issue, which is available at wileyonlinelibrary.com.]

were attributed to the leucoemeraldine–emeraldine I, emeraldine I–emeraldine II, and emeraldine II–pemigraniline transformation, respectively.[35] A possible transformation was shown in Scheme 3. In addition, the CV curves of P(FcA-*co*-ANI) were compared with those of PANI. It was obvious that the P(FcA-*co*-ANI) possessed a higher peak than PANI. Meanwhile, two pairs of conspicuous peaks appeared in the CV curves of PANI. The results suggest that the structure of Fc in the main chain promoted the capacitance of P(FcA-*co*-ANI).

Furthermore, CV of the copolymer was measured at scanning rates from 5 to 200 mV/s. As shown in Figure 11, the relationship between the scanning rate and peak current density was

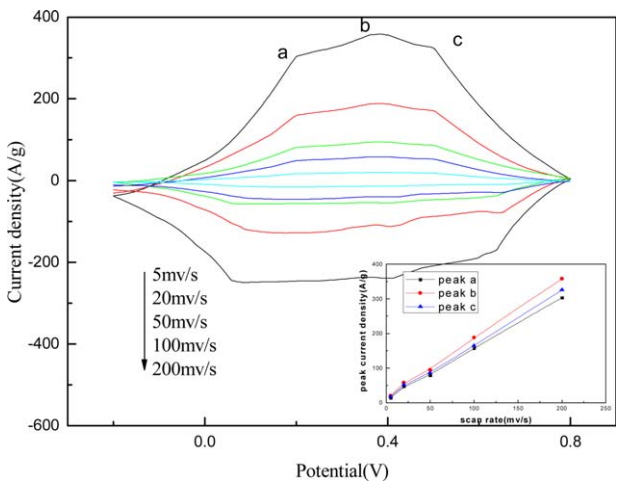

Figure 11. CV curves of P(FcA-*co*-ANI) at different scan rates. [Color figure can be viewed in the online issue, which is available at wileyonlinelibrary.com.]

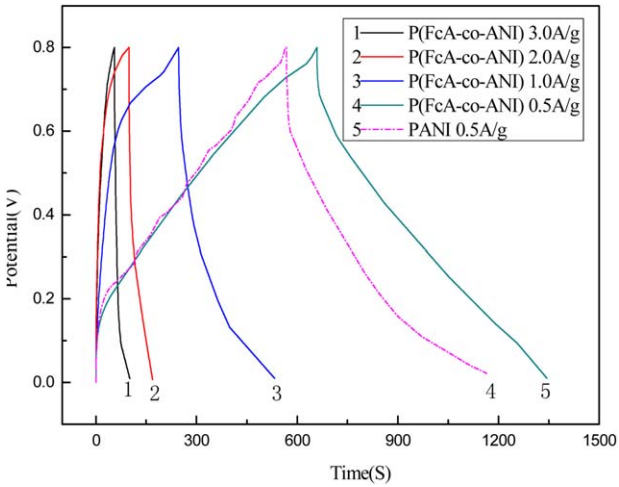

Figure 12. Charge–discharge curves of P(FcA-*co*-ANI) at different current densities and PANI at 0.5 A/g. [Color figure can be viewed in the online issue, which is available at wileyonlinelibrary.com.]

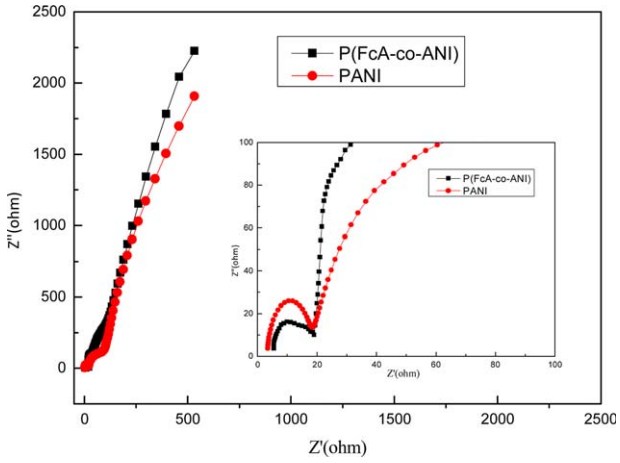

Figure 14. EIS of P(FcA-*co*-ANI) and PANI. Z′ was the real part of alternating current impedance, Z″ was the imaginary part of alternating current impedance. [Color figure can be viewed in the online issue, which is available at wileyonlinelibrary.com.]

nearly linear. The shape of the curve was a polygon in the given potential range (from −0.2 to 0.8 V).

The charge–discharge curves are depicted in Figure 12. The results show that the copolymer had good capacitive behavior at large-scale current densities because of the nearly symmetric charge–discharge curves. The capacitance of P(FcA-*co*-ANI) was up to 433.1 F/g and was superior to the capacitance of PANI (373.8 F/g) when the current density was 0.5 A/g. Furthermore, C_s was still 187.6F/g when the current density was increased to 3 A/g; this was ascribed to the fact that the redox reaction rate and charge diffusion could not keep pace with the rapid change in the potential. This result was explained as following. First, the main chain of the copolymer had ferrocenyl with electron-rich properties. Second, the π-conjugated structure and short conjugated segment enhanced the electron transport and shortened the electrolyte ion-transmission paths.

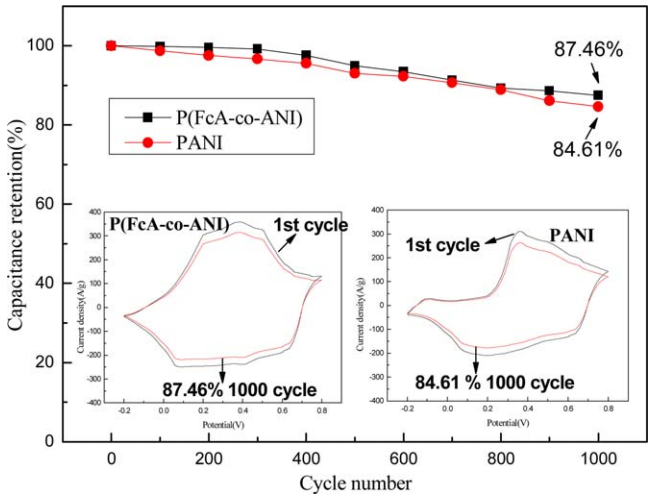

Figure 13. Cyclic performance of P(FcA-*co*-ANI) and PANI at 0.5A/g for 1000 cycles. [Color figure can be viewed in the online issue, which is available at wileyonlinelibrary.com.]

Cycling performance testing was carried out at a current density of 0.5 A/g. As shown in Figure 13, P(FcA-*co*-ANI) presented satisfactory cycling stability after 1000 cycles, and C_s retained a value of 87.46%, which was better than that of PANI (84.61%). This was mainly due to the degree of molecular regularity being affected by ferrocenyl in the main chain.

As shown in Figure 14, EIS was measured in the frequency range from 10^5 to 10^{-2} Hz. The Nyquist plots of P(FcA-*co*-ANI) and PANI were an almost semicircle in the high-frequency region and a line almost straight from the real axis in the low-frequency region, respectively. The verticality of the copolymer was better than that of PANI. The intercepts of the curves of the copolymer indicated the contact resistance was 5.2 Ω, and that of PANI was 3.6 Ω. The interracial charge-transfer resistance was calculated with the diameter of the semicircle.[36,37] The charge-transfer resistance of P(FcA-*co*-ANI) was 13.5 Ω, which was smaller than that of PANI (15.6 Ω).

CONCLUSIONS

A novel electroactive copolymer with a special structure was prepared through simple electrochemical polymerization. The structure of the monomer and copolymer were evaluated from FTIR spectroscopy, ^{1}H-NMR, XRD, and SEM. The results showed that FcA existed as hyperconjugation forms, this gave the copolymer excellent electrochemical properties. The effects of the monomer molar ratios and scan rate were examined to gain the optimal synthesis conditions of the copolymer. The C_s of P(FcA-*co*-ANI) was as high as 433.1 F/g at 0.5 A/g, and the internal resistance was small enough. The electrochemical properties of the copolymer were studied in detail. The results showed that three redox transformations appeared in the CV curve of the copolymer, furthermore, the C_s of P(FcA-*co*-ANI) was superior to that of PANI. The diffusion resistance was very small, and the durability was good enough. Therefore, P(FcA-*co*-ANI) could be used for the development of new conducting polymers.

ACKNOWLEDGMENTS

This work was financially supported by the Natural Science Foundation of Fujian Province (contract grant number 2014J01386) and the Pride Youth Program of Fujian Provincial High Education (contract grant number JA12409).

REFERENCES

1. Rudge, A.; Davey, J.; Raistrick, I.; Gottesfeld, S. *J. Power Sources* **1994**, *47*, 89.
2. Dubal, D. P.; Patil, S. V.; Kim, W. B.; Lokhande, C. D. *Mater. Lett.* **2011**, *65*, 2628.
3. Woo, S. W.; Dokko, K.; Kanamura, K. J. *Power Sources* **2008**, *185*, 1589.
4. Li, H.; Wang, J.; Chu, Q.; Wang, Z.; Zhang, F.; Wang, S. *J. Power Sources* **2009**, *190*, 578.
5. Zhang, J.; Kong, L. B.; Li, H.; Luo, Y.-C; Kang, L. *J. Mater. Sci.* **2010**, *45*, 1947.
6. Zhang, L. L.; Zhao, S. Y.; Tian, X. N.; Zhao, X. S. *Langmuir* **2010**, *26*, 17624.
7. Mujawar, S. H.; Ambade, S. B.; Battumur, T.; Ambade, R. B.; Lee, S.-H. *Electrochim. Acta* **2011**, *56*, 4462.
8. Murugan, C.; Subramanian, E.; Padiyan, D. P. *Sens. Actuators B* **2014**, *205*, 74.
9. Peng, X. Y.; Liu, X. X.; Hua, P. J.; Diamond, D.; Lau, K. T. *J. Solid State Electrochem.* **2010**, *14*, 1.
10. Pina, C. D.; Ferretti, A. M.; Ponti, A.; Falletta, E. *Compos. Sci. Technol.* **2015**, *110*, 138.
11. Wu, J. C.-C.; Ray, S.; Gizdavic-Nikolaidis, M.; Uy, B.; Swift, S.; Jin, J.; Cooney, R. P. *Synth. Met.* **2014**, *198*, 41.
12. Borah, R.; Banerjee, S.; Kumar, A. *Synth. Met.* **2014**, *197*, 225.
13. Depa, K.; Strachota, A.; Stejskal, J.; Bober, P.; Cimrová, V.; Prokeš, J.; Trchová, M.; Šlouf, M.; Hodan, J. *J. Appl. Polym. Sci.* **2015**, *132*, 1.
14. Adams, P. N.; Apperley, D. C.; Monkman, A. P. *Polymer* **1993**, *34*, 328.
15. Wright, A. M. K.; Feast, W. J.; Adams, P. N.; Milton, A. J.; Monkman, A P. *Polymer* **1992**, *33*, 4292.
16. Grgur, B. N.; Elkais, A. R.; Gvozdenovića, M. M.; Drmanića, S. Ž.; Trišovićb, T. Lj.; Jugović, B. Z. *Prog. Org. Coat.* **2015**, *79*, 17.
17. Yu, L.; Gan, M.; Ma, L.; Huang, H.; Hu, H.; Li, Y.; Tu, Y.; Ge, C.; Yang, F.; Yan, J. *Synth. Met.* **2014**, *198*, 167.
18. Liu, H.; Zhang, W.; Song, H.; Chen, X.; Zhou, J.; Ma, Z. *Electrochim. Acta* **2014**, *146*, 511.
19. Baniasadi, H.; Ramazani, S. A. A.; Mashayekhan, S.; Ghaderinezhad, F. *Synth. Met.* **2014**, *196*, 199.
20. Varma, S. J.; Jayalekshmi, S. *J. Appl. Polym. Sci.* **2010**, *117*, 138.
21. Torriero, A. A. J. *Electrochim. Acta* **2014**, *137*, 235.
22. Hu, K.; Xu, B.; Shao, H. *Electrochem. Commun.* **2015**, *50*, 36.
23. Hernández-Muñoz, L. S.; Galano, A.; Astudillo-Sánchez, P. D.; Abu-Omar, M. M.; González, F. J. *Electrochim. Acta* **2014**, *136*, 542.
24. Alkan, A.; Natalello, A.; Werre, M.; Frey, H. *Macromolecules* **2014**, *47*, 2242.
25. Bicil, Z.; Camurlu, P.; Yucel, B.; Becer, B. *J. Polym. Res.* **2013**, *20*, 228.
26. Friebe, C.; Hager, M. D.; Winter, A.; Schubert, U. S. *Adv. Mater.* **2012**, *24*, 332.
27. Çılgı, G. K.; Karakus, M.; Ak, M. *Synth. Met.* **2013**, *180*, 25.
28. Crepaldi, L. B.; Neto, S. A.; Cardoso, F. P.; Ciancaglini, P.; De Andrade, A. R. *Electrochim. Acta* **2014**, *136*, 52.
29. Sung, D.; Yang, S. *Electrochim. Acta* **2014**, *133*, 40.
30. Chao, D.; Lu, X.; Chen, J.; Liu, X.; Zhang, W.; Wei, Y. *Polymer* **2006**, *47*, 2643.
31. Leppänen, A.-S.; Xu, C.; Liu, J.; Wang, X.; Pesonen, M.; Willför, S. *Macromol. Rapid Commun.* **2013**, *34*, 1056.
32. Venancio, E. C.; Mattoso, L. H. C.; Motheo, A. J. J. *Braz. Chem. Soc.* **2001**, *12*, 526.
33. Lu, X. F.; Gao, H.; Chen, J. Y.; Chao, D. M.; Zhang, W.; Wei, Y.; Trišovićb, T.Lj.; Jugović, B. Z. *Nanotechnology* **2005**, *16*, 113.
34. Sengupta, P. P.; Kar, P.; Adhikari, B. *Bull. Mater. Sci.* **2011**, *34*, 261.
35. Wu, Q.; Xu, Y.; Yao, Z.; Liu, A.; Shi, G. *ACS Nano* **2010**, *4*, 1963.
36. Rajeswari, J.; Kishore, P. S.; Viswanathan, B.; Varadarajan, T. K. *Electrochem. Commun.* **2009**, *11*, 572.
37. Li, X.; Rong, J.; Wei, B. *ACS Nano* **2010**, *4*, 6039.